hydrology

MDPI

Article

Hydrodynamic Modeling as a Decision-Support Tool for Coastal Management in Large Amazonian Estuaries: A Case Study in the Pará River System, Brazil

Ana Hilza Barros Queiroz *, Marco Antônio Vieira Callado †, Iago Vasconcelos Gadelha Barbosa ‡, Thaís Angélica da Costa Borba and Marcelo Rollnic

Marine Environmental Monitoring Research Laboratory (LAPMAR), Federal University of Pará, Augusto Corrêa Street 01-Guamá, Belém 66075-110, PA, Brazil; mavcallado@gmail.com (M.A.V.C.); iagogadelhab@gmail.com (I.V.G.B.); tacborba@gmail.com (T.A.d.C.B.); rollnic@ufpa.br (M.R.)

* Correspondence: anahbqueiroz@gmail.com

† Current address: Oceanographic Institute of the University of São Paulo (IOUSP), University of São Paulo, Oceanographic Square 191, São Paulo 05508-120, SP, Brazil.

‡ Current address: Ocean Dynamics Laboratory (LABDINO), Federal University of Santa Catarina, Campus Universitário Reitor João David Ferreira Lima Trindade, Florianópolis 88040-900, SC, Brazil.

Abstract

Tropical estuaries are socioeconomically important yet highly vulnerable environments. In the eastern Amazon, the Pará River Estuary (PRE) and adjacent water bodies support the city of Belém and are increasingly affected by environmental pressures but remain underrepresented in numerical modeling efforts. The influence of key input parameters on hydrodynamic model performance in these systems remains poorly characterized, hindering the development of reliable simulation tools for this region. We present the calibration and validation of a two-dimensional hydrodynamic model for the PRE, Guajará Bay, and the Guamá River, examining how parameters such as bathymetry, roughness, and tidal and discharge forcings influence model performance. Delft3D-FM was applied using tidal harmonics and seasonal river discharge as primary forcings, with model skill evaluated against observed water levels and discharge across ten seasonally distinct scenarios over seven calibration iterations. Tidal forcing and bathymetric representation emerged as the dominant performance drivers: replacing global tidal datasets with locally derived harmonics substantially reduced simulation errors, and bathymetric refinements also improved discharge representation. Final performance met established satisfactory thresholds at the majority of observation points and cross-sections. The calibrated model provides a basis for investigating processes governed by local hydrodynamics, such as water quality assessments, contaminant dispersion, and infrastructure planning.

Keywords: calibration; Amazon; estuary; Delft3D-FM

Check for updates

Academic Editor: Carlo Gualtieri

Received: 11 May 2026
Revised: 3 June 2026
Accepted: 7 June 2026
Published: 11 June 2026

Copyright: © 2026 by the authors. Licensee MDPI, Basel, Switzerland. This article is an open access article distributed under the terms and conditions of the Creative Commons Attribution (CC BY) license.

1. Introduction

The Amazon region is recognized for its vast spatial extent, environmental complexity and global and regional significance. The Amazon River discharges large volumes of water and sediments into the Atlantic Ocean, supporting biological productivity on the continental shelf and transporting dissolved substances and particulate matter from the continent into the ocean [1]. Its extensive hydrographic network sustains diverse ecosystems and supports socioeconomic activities developed along local rivers and estuaries, such

as fishing, navigation and tourism [2–4]. These waters are central to Amazonian culture, with many communities depending on them for their livelihoods [5–7].

Managing these waters is therefore crucial to both environmental quality and local livelihoods. Sustainable management requires understanding how tidal–fluvial dynamics control water renewal and the transport and retention of sediments and contaminants. Additionally, climate-change impacts (e.g., more frequent floods) combined with ongoing coastal pressures further increase the need for process-based knowledge to inform monitoring design, risk assessment and the evaluation of management options.

Hydrodynamic models play an important role in this context, as they enable the evaluation and visualization of physical processes across different spatial and temporal scales—including hard-to-reach environments with complex hydrodynamics [8,9]—and provide the foundation for water quality simulations [10]. Such tools can be used to assess litter, pollutant transport and retention [11,12], predict oil-spill dispersion [13], support the planning of new ventures in the coastal zone [14], and evaluate potential impacts from the installation of structures (e.g., ports) [15,16].

A well-calibrated model is fundamental for informed decision-making as it helps avoid unnecessary interventions and supports the identification of more sustainable alternatives based on accurate and reliable data [17,18]. This is particularly important in complex environments such as the Amazon—characterized by a vast network of large rivers and numerous smaller channels that exert significant influence on local hydrodynamics, in addition to the pronounced action of macrotides—whose scale and complexity can impede the rapid development of reliable simulation tools.

Calibration and validation are crucial steps for the effective application of hydrodynamic models in regional studies. These processes aim to adjust pre-selected parameters, which must be representative of local hydrodynamics, within the computational limitations and inherent simplifications of the model, ensuring the most accurate representation of the physical environment possible [19]. They also allow the influence of individual parameters on model behavior to be assessed, highlighting those that exert greater control over system dynamics. These tasks are especially challenging in large domains, where validation requires extensive, high-quality observational data for input and comparison purposes [20].

Within the Amazon coastal zone, several estuarine systems remain poorly represented in numerical modeling studies, despite their environmental and socioeconomic importance. The Pará River Estuary, together with the Guamá River and Guajará Bay, forms one of the major tidal–fluvial systems of the eastern Amazon and represents a typical example of the complex hydrodynamic environments found along the Amazon coast. Despite their importance, the influence of key model inputs on hydrodynamic performance, as well as the large-scale hydrodynamic behavior of these systems, remains relatively underexplored.

Given this scenario, the present study aims to develop a hydrodynamic simulation for the Pará River Estuary, the Guamá River, and Guajará Bay—located in the vicinity of the city of Belém, the capital of the state of Pará. We examine how parameters associated with tidal forcing, river discharge, roughness, and bathymetry influence model performance and assess the extent to which locally derived data improve simulation skill. The calibrated model contributes to improving hydrodynamic representation in macrotidal Amazonian estuaries, deepens understanding of modeling processes in complex tropical estuaries and is expected to support future water quality studies.

2. Materials and Methods

2.1. Study Area

The study region is located within the Amazon Coastal Zone, characterized by complex hydrodynamics due to a combination of different forcing mechanisms, such as the

macrotidal regime and intense river discharges (Figure 1). The estuary is governed by semidiurnal meso- (upstream of the system) to macrotides, presenting the semidiurnal M2 and S2 as the main harmonic components, alongside the emergence of secondary components M4 and Msf, which become more pronounced as the tidal wave propagates into the estuary [21].

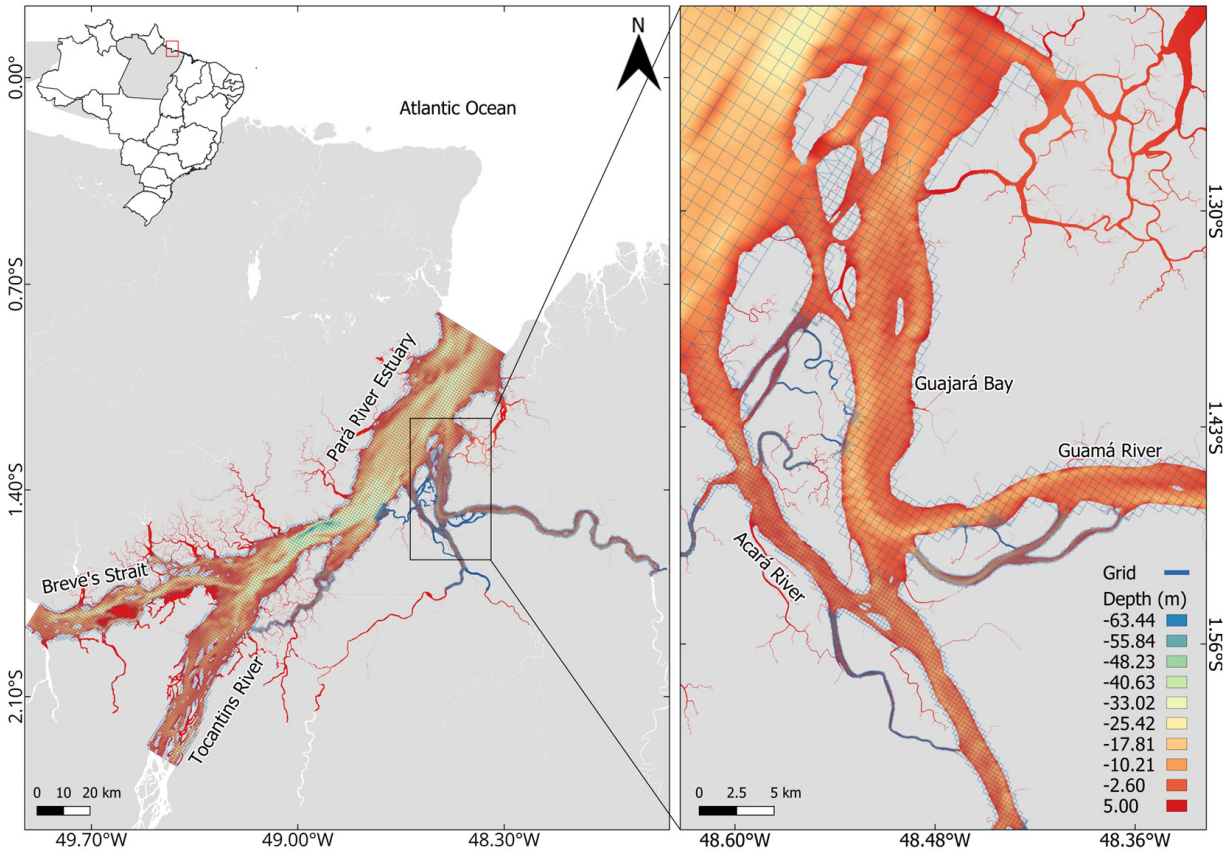


Figure 1. Map of the study area, including unstructured grid and bathymetric values, with a detailed view of the Guajará Bay and Guamá River region.

In this system, three water bodies stand out in the vicinity of Belém: the Guamá River, Guajará Bay, and the Pará River Estuary (Figure 1). The Pará River flows into the Atlantic Ocean with a mean annual discharge on the order of magnitude of 10^4 $m^3 \cdot s^{-1}$, connected to the Amazon River via the Breves Strait and having the Tocantins River as its main tributary [22].

Guajará Bay is located on the right bank of the estuary; it is characterized by a predominantly muddy bottom, a maximum water level variation of 3.6 m, and positive tidal asymmetry [23]. The Guamá River empties into the bay, sharing similar tidal characteristics and substrate types with the bay itself [23,24].

According to the Köppen climate classification, the region presents climate classes Af, Am, and Aw—tropical rainforest, tropical monsoon, and tropical savanna climates, respectively [25]—with mean annual temperatures of 26 °C and precipitation of 3001 mm. Seasons in the region are divided into the rainy season (December to July) and the dry season (July to December). March is the month with the highest precipitation, averaging 359 mm of rain, while October is the driest, averaging 40 mm [26]. Wind direction shows low seasonal variability, being predominantly easterly. The highest wind speeds occur from August to January, averaging above 5.3 km/h, while the lowest magnitudes occur from January to August, at 4.2 km/h [26].

2.2. Model Setup

Delft3D-FM Suite 2019.01, developed by Deltares, was chosen to run the simulations for the study area. The model solves the Navier–Stokes equations under shallow waters and Boussinesq assumptions in one, two and three dimensions on unstructured horizontal grids. It simulates flow and transport processes driven by tidal and meteorological forcing and is commonly applied to studies in coastal environments, such as estuaries [27], with previous successful applications to the Pará River Estuary and Amazon River [28,29].

2.2.1. Domain

The domain was defined to extend beyond the study's focus area, aiming to minimize intrinsic errors arising from the model's open boundaries [20]. The mesh was constructed following the high-tide coastline obtained from the Marine Environmental Monitoring Research Laboratory (LAPMAR) and the Amazon Coastal Observatory (OCA). Quadrangular elements of varying resolutions—ranging from 1000 × 1000 m to 20 × 20 m—were configured and connected by triangular cells to form an unstructured mesh totaling 20,991 cells and covering approximately 7000 km^2 (Figure 1).

This approach allowed for reduced computational effort due to the use of lower-resolution cells in more extensive water bodies, such as the Pará River, which is 50 km wide at its mouth. Conversely, it allowed finer resolution in the study's focal region, including small local channels.

2.2.2. Morphology

The bathymetry interpolated to the domain was acquired from the LAPMAR and OCA databases. Interactions between water bodies and adjacent floodplains were disregarded by raising the elevation of cells located along the coastline by 5 m (Figure 1). Depth values were interpolated to net nodes and cell faces by the simple averaging method, which calculates the mean depth value from samples located inside each cell [27].

Roughness was calculated using the Manning coefficient, following the methodology proposed by [30]. This equation combines a base value for bottom material (n_b), a correction factor for surface irregularities (n_1), a value for variations in the channel's cross-section (n_2), a value for obstructions (n_3) and vegetation (n_4), as well as a correction factor for the meandering degree of the channel (m):

$$n = (n_b + n_1 + n_2 + n_3 + n_4)m$$

The same interpolation method used for bathymetric data was applied, with the highest values (0.039) assigned near the mouth of Guajará Bay, at Cotijuba Island, while the lowest values (0.020) were located in the Acará River and the upstream portion of the Guamá River (Figure 2, Table 1).

Table 1. Manning's roughness parametrization applied to the final model configuration.

Region	n_b	n_1	n_2	n_3	n_4	m	n
Upstream of the Guamá and Acará rivers	0.012	0.001	0.001	0.001	0.002	1.2	0.020
Guajará Bay and downstream of the Acará River	0.017	0.002	0.001	0.001	0.002	1	0.023
Downstream portion of the Pará River Estuary	0.017	0.003	0.003	0.003	0.003	1	0.029
Upstream portion of the Pará River Estuary	0.022	0.004	0.002	0.003	0.002	1	0.033
Tocantins River	0.023	0.004	0.002	0.005	0.002	1	0.036
Cotijuba Island	0.028	0.004	0.001	0.004	0.002	1	0.039

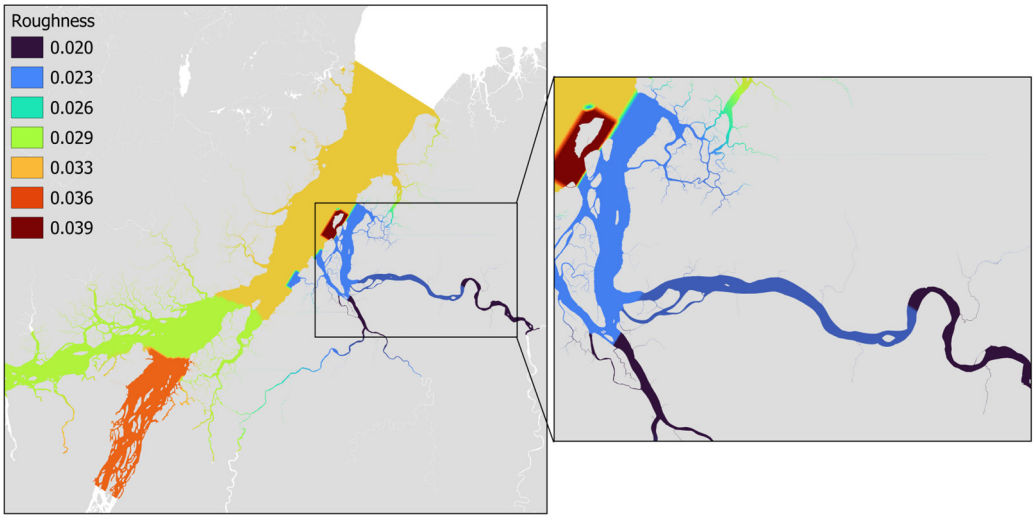


Figure 2. Domain roughness map.

2.2.3. Boundary Conditions

The simulation used tides and river discharge as the primary hydrodynamic forcings. These were chosen due to their significant influence on local hydrodynamics and their ability to modify the landscape of the Amazon Estuary [31,32].

Tides were configured at the open boundaries corresponding to the mouth of the Pará River at the northern limit, and the Breves Strait at the southern limit (Figure 3). The first boundary was driven by 60 harmonic components extracted from data collected by LAPMAR near the city of Colares over a two-year period; M2 displayed the greatest amplitude (1.65 m), followed by S2 (0.41 m). The second boundary was configured using 13 components generated by the TPXO 7.2 Tidal Model—part of the DelftDashboard tool—which has previously been applied in studies of the region [28,29]. As the latter is located further into the estuary, the components with the largest amplitudes were N2, P1 and Q1 with 0.9, 0.5 and 0.5 m, respectively.

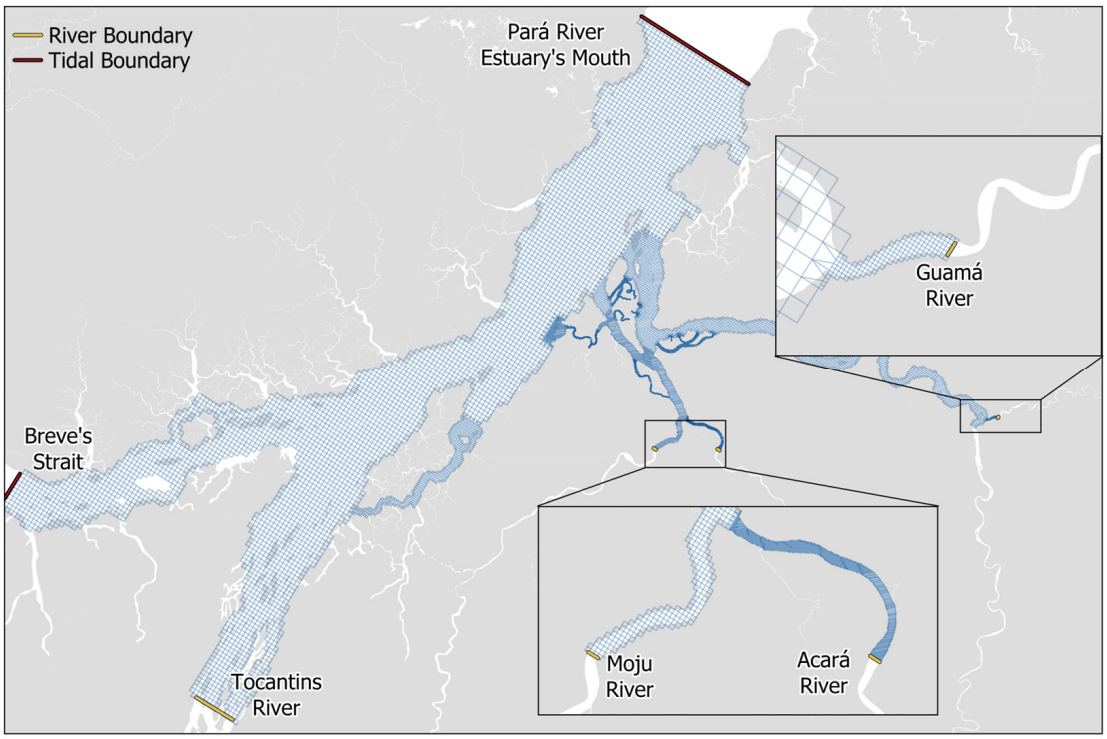


Figure 3. Map showing the location of tidal and river discharge open boundaries.

River discharge was configured for the boundaries located at the Tocantins, Moju, Acará, and Guamá rivers (Figure 3). Each boundary was forced with discharge values derived from empirical calculations using historical time series data from the Tocantins and Guamá rivers, obtained from the National Water Agency (ANA) (Table 2). The calculation accounted for the distance between the original gauging stations and the simulation boundaries, resulting in the application of a $\times 10$ factor for the original Guamá River values, and $\times 2$ for the Tocantins River.

Table 2. ANA's hydrometric stations used for collecting raw instant discharge data for river boundaries.

River	Station Name	Station ID	Data Interval
Tocantins	Tucuruí	29700000	1969–2016
Guamá	Bom Jardim	31520000	1964–2022

In the absence of historical discharge records for the Acará and Moju rivers, their discharge was estimated from the Guamá River time series. This approach is supported by the shared hydrological setting of the three rivers within the Guamá–Moju watershed [23], which imposes the same precipitation regime, land cover, and runoff dynamics across all sub-catchments. The drainage areas of the Guamá, Acará, and Moju are of the same order of magnitude (10^4 km^2) [33–35], further supporting the proportional transfer of the discharge signal. Additionally, all three rivers share comparable tidal characteristics in their lower reaches, including semidiurnal macrotidal forcing and positive tidal asymmetry [24]. In this context, factors of 5 and 1 were applied to the Acará and Moju boundaries, respectively. Final discharge values, after further calibration attempts, are displayed in Figure 4.

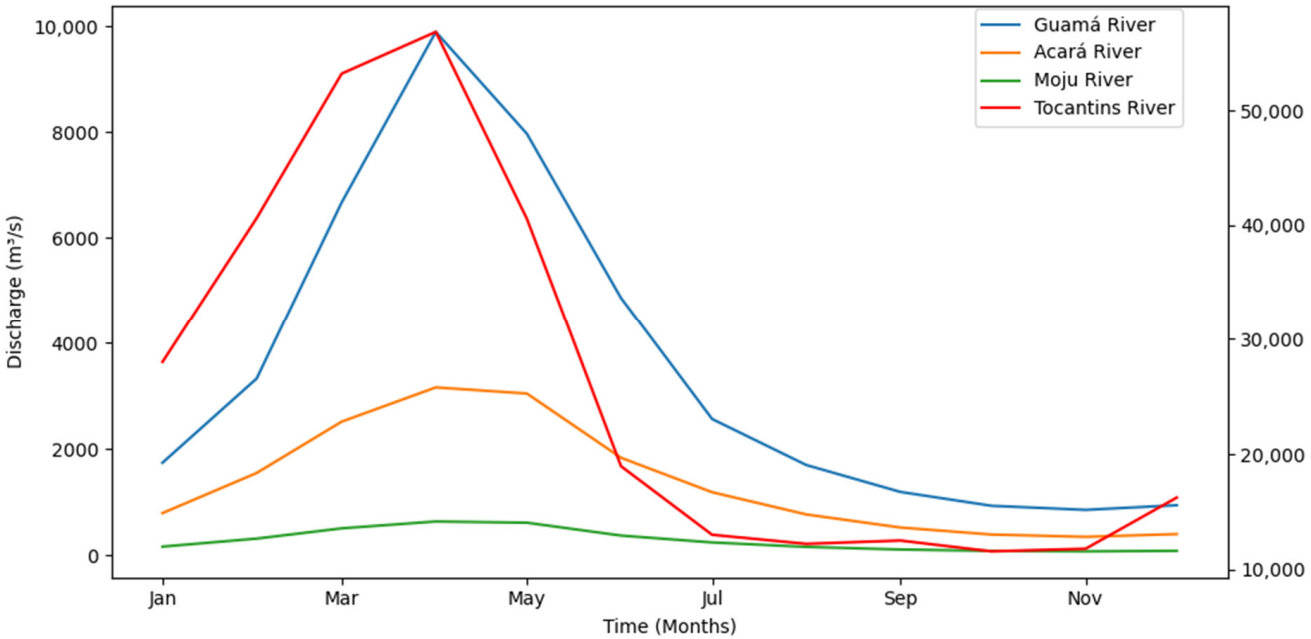


Figure 4. Final river discharge values (m^3/s) for the open boundaries of the Tocantins (right *y* axis), Guamá, Acará, and Moju rivers (left *y* axis).

Free surface elevation and river discharge were selected as parameters to evaluate simulation performance due to their importance to the region's dynamics. This analysis was performed using the Pearson correlation coefficient (r), the Nash–Sutcliffe efficiency coefficient (NSE), and the Percentage Root Mean Square Error (pRMSE). These indices were selected due to their frequent use in assessing hydrodynamic simulations [20,32,36], as well as their previous application in studies of this region [28,29]. The performance

thresholds were adopted from [20,37–39]: r > 0.9; NSE > 0.5; and pRMSE < 10% for free surface elevation and <20% for river discharge.

$$r = \frac{\sum_{i=1}^{N} (S_i - \overline{S}_i)(O_i - \overline{O}_i)}{\sqrt{\sum_{i=1}^{N_i} (S_i - \overline{S}_i)^2} \sqrt{\sum_{i=1}^{N_i} (O_i - \overline{O}_i)^2}}$$

$$NSE = 1 - \frac{\sum_{i=1}^{N} (O_i - S_i)^2}{\sum_{i=1}^{N} (O_i - \overline{O})^2}$$

$$pRMSE = 100 \frac{\sqrt{\left(\frac{1}{N}\right) \sum_{i=1}^{N} (O_i - S_i)^2}}{O_{max} - O_{min}}$$

where O_i and S_i are the observed and simulated values, respectively; $\overline{O}$ and $\overline{S}$ are the mean observed and simulated values for the scenario evaluated, respectively; O_{max} and O_{min} are the maximum and minimum observed values; and N is the number of samples.

The combined use of r, NSE, and pRMSE provides a comprehensive assessment of model performance by evaluating complementary aspects of the agreement between observed and simulated data. Pearson's r indicates how well the model reproduces the timing and variability of the observed signal; pRMSE quantifies the magnitude of the differences between observations and simulations, providing a direct measure of overall error; and NSE complements these metrics by simultaneously accounting for variance reproduction, amplitude deviations, and systematic bias relative to the observed series [40]. The combined interpretation of r, NSE, and RMSE allows for a robust diagnostic evaluation of model performance, encompassing correlation, error magnitude, and bias-related effects. Because systematic overestimation, underestimation, and amplitude discrepancies are already reflected in NSE and RMSE values, the inclusion of a separate mean-bias metric would provide largely redundant information and would not substantially alter the interpretation of the model results.

The analysis was performed at 10 observation points (P) for water level and 13 cross-sections (CS) for discharge (Figure 5), coinciding with in situ data collection sites monitored by LAPMAR. Ten distinct scenarios were simulated, covering various seasonal periods (Table 3). The use of multiple scenarios, across varying seasonal and interannual periods, provides a robust assessment of model behavior under different regimes, turning the calibration process itself into an intrinsic, robust validation of model performance. Therefore, model calibration and validation are treated as a single process in this study.

Table 3. Scenarios simulated during model calibration.

Scenario	Corresponding Month/Year	Discharge Condition
S1	June/2013	Transition to low discharge
S2	October/2015	Low discharge
S3	March/2019	High discharge
S4	October/2019	Low discharge
S5	May/2021	Transition to low discharge
S6	January/2022	Transition to high discharge
S7	April/2022	High discharge
S8	July/2022	Transition to low discharge
S9	October/2022	Low discharge
S10	April/2023	High discharge

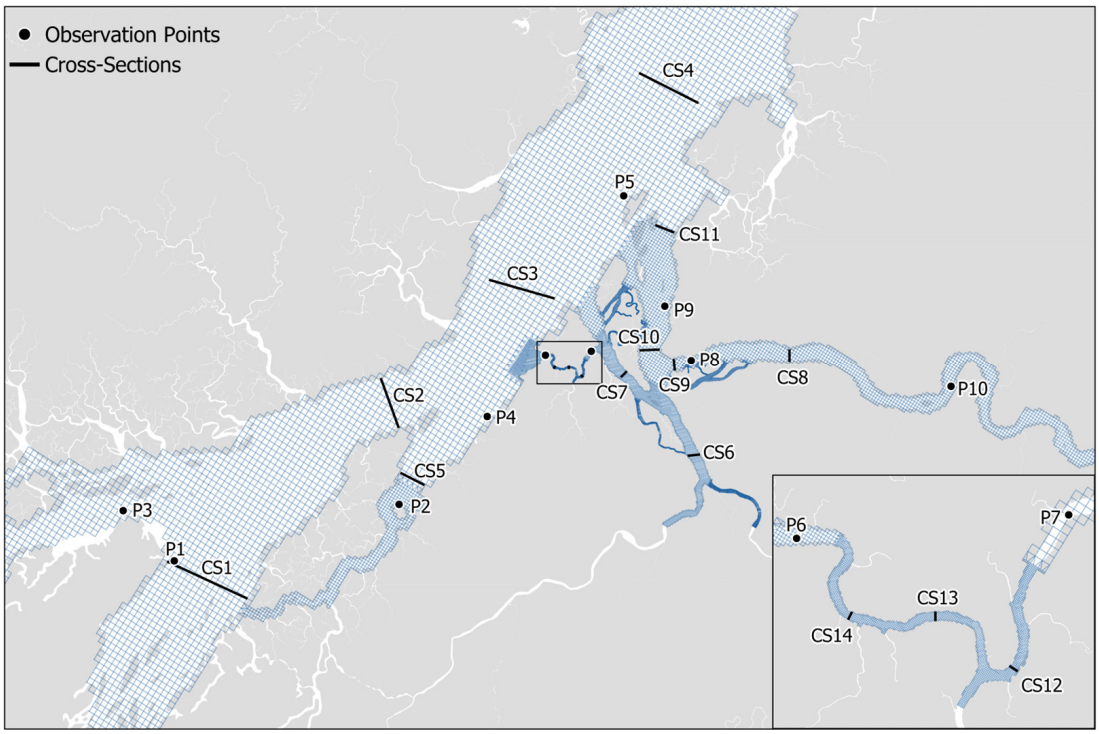


Figure 5. Location of observation points and cross-sections used during the calibration and validation processes.

The process followed a trial-and-error approach [41], involving the adjustment of bathymetry, roughness, river discharge, and the amplitude of harmonic components, all of which are common sources of errors [32,42–44]. The rationale for each adjustment and the interpretation of the resulting changes in model performance is discussed in Section 4.

3. Results

The calibration and validation process was carried out over seven iterations (V1 to V7), during which all observation points and cross-sections were analyzed; that is, the 10 scenarios proposed for calibration were simulated in each iteration. Time series comparisons between simulated and observed water level and river discharge were plotted for all scenarios and are provided in Appendices A and B, respectively.

Various parameters were adjusted to improve simulation efficiency: the most impactful changes were adjustments to harmonic components and increased river discharge values for the Guamá, Acará, and Moju rivers, besides the adjustments to the depth of these channels. A description of the main modifications implemented and their corresponding results are presented in Table 4.

Overall, the implemented modifications ensured that the simulation reproduced the hydrodynamic phenomena of the study area satisfactorily on a global scale, as indicated by the final validation indices.

Regarding tides, pRMSE values below 10% were observed for almost all points at V7, particularly those located within the study's focal area (Figures 6 and A1). Only points P3 and P10 presented values above the satisfactory threshold, though still close to the desired 10%. For the r and NSE, results exceeded the minimum requirements at all points.

Furthermore, all points displayed great improvement from V5 onwards, with this scenario yielding the best values for all parameters (Figure 6). However, the adjustments in V6 and V7—aimed at improving river discharge simulation—caused a slight increase in water level error, but not beyond the upper limit of the satisfactory interval (Figure A1).

Table 4. Calibration attempts and results for the 7 iterations required to achieve optimal model efficiency.

Iteration	Main Modifications	Results
V1	Uniform roughness (0.023); original calculated discharge values; both tidal inputs generated by the TPXO 7.2 model.	Indices became significantly above ideal levels for free surface elevation and velocity field.
V2	Variable roughness; 10% increase in river discharge for all sections; increased amplitude for M2, S2, and MN4 components.	Increase in pRMSE for almost all points and sections.
V3	Reduction in roughness values; return to original component amplitude values, with a 0.5 m increase in M2; 50% increase in calculated Guamá River discharge; deepening of areas near cross-sections by 1 m.	Significant improvement at some tide points (e.g., P8 and P9) and sections in the study's focal region.
V4	Roughness reduction in the Guamá and Acará rivers and increase in the rest of the domain; return to original bathymetry; 20% increase in river discharge compared to original values—except for the Guamá River.	Error increased at most points and sections.
V5	Replacement of the TPXO 7.2 tidal input with Colares data at the mouth of the Pará River Estuary; downstream extension of the grid in the Acará and Moju rivers; 5-fold increase in Guamá River discharge and deepening of the region by 2 m.	Global error reduction, attributed mainly to the change in tidal input. Scenario S5 showed an increase in error at CS8 and CS9.
V6	Increase in M2 component by 0.3 m; 1 m depth reduction in the Acará and Guamá river regions; doubled river discharge original values for the Acará, Guamá, and Moju rivers.	Considerable error reduction in cross-sections; slight increase in pRMSE for observation points, but within acceptable intervals.
V7	Increased roughness near section CS3.	Error reduction at this section.

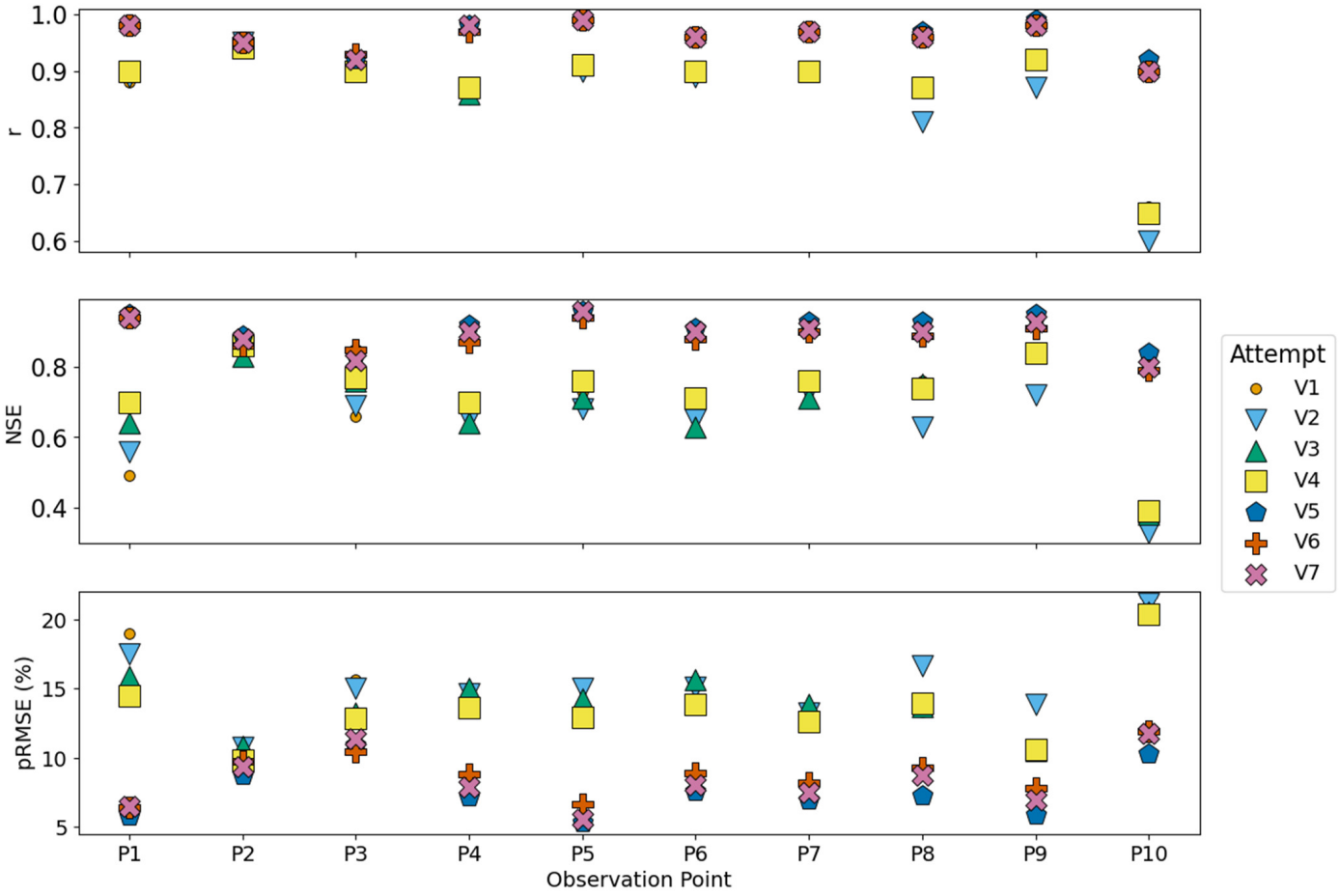


Figure 6. Validation index values for water level across calibration attempts 1 through 7.

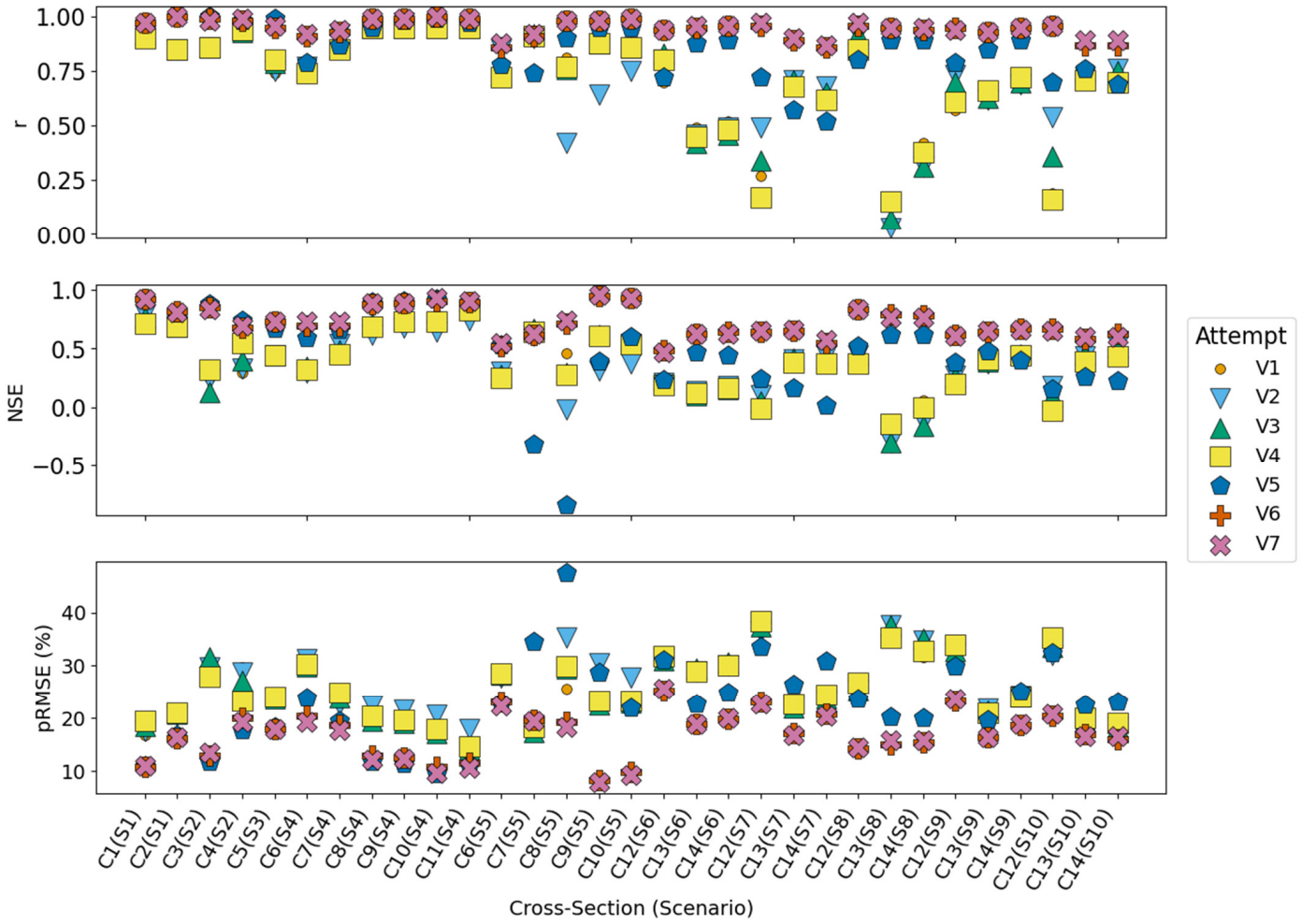


Figure 7. Validation index values for river discharge across calibration attempts 1 through 7.

River discharge also yielded satisfactory results at V7, with the lowest pRMSE values observed in the Guajará Bay and Guamá River area (Figures 7 and A2–A4), indicating high simulation efficiency in a region of significant interest for the study. In contrast, values falling outside the satisfactory range were found in the Acará River and Furo do Arrozal—a result that was mirrored in the r and NSE indices.

Once more, a great improvement was observed from V5 onwards. However, differing from the water level calibration, V7 is the iteration with the best indices, as the parameters were adjusted to improve discharge simulation despite the slight increase in water level error. Scenarios of low discharge or transition to low discharge showed less indices above the satisfactory threshold (Figures A2 and A4), while high-discharge scenarios presented slightly higher final indices (Figure A3).

4. Discussion

This simulation involved numerous challenges stemming from the complexity of the study region, which is representative of many environments across the Amazonian coastal system. The large spatial extent required several calibration stations and fine grid resolution to account for the varying channel sizes and geometry in the domain. Validation metrics had to be balanced to guarantee global efficiency and to establish this model as adequate for further applications (e.g., water quality, particle transport) and as a tool for understanding the hydrodynamics of the Pará River Estuary and tributaries that influence the city of Belém (Pará), Brazil.

The calibration and validation results demonstrated that reliable modeling for complex estuaries, such as the Pará River, depends on the use of locally acquired data. However, many of these environments remain poorly monitored, whether within the Amazon [2,45,46] or across the globe [47,48]. Data acquisition is often limited, particularly in developing regions where financial and human resources for large-scale environmental monitoring are scarce.

Previous hydrodynamic models developed for this region focused primarily on the Amazon and Pará rivers at larger spatial scales, with limited calibration coverage in the Guajará Bay and Guamá River area [28]. By incorporating a denser observational network and extending the validated domain upstream into the Guamá and Acará rivers—both of which exert significant influence on Guajará Bay dynamics—the present study not only matched the performance indices reported by Borba et al. [28] but demonstrated satisfactory skill across a broader portion of the domain. Regional studies using comparable observation stations reported stronger performance metrics in the vicinity of the bay but lower skill in the upstream estuarine reaches [32,42]. Crucially, those studies did not include river discharge as a validation variable for most of the Pará River Estuary. Incorporating discharge validation in the present study imposed an additional calibration constraint that required adjustments, which in turn produced a marginal increase in water level error in the final iterations. This trade-off was a deliberate modeling choice, where we prioritized a balanced, domain-wide representation of both water level and discharge.

The comparison between modeled and observed series indicated good to excellent performance for both water level and discharge, mainly because of modifications to bathymetry and boundary conditions. By improving the representation of water levels and river discharge, the calibrated model provides a robust foundation for applications in water quality and transport processes and established it as a tool for visualizing estuarine surface flow. This supports understanding of local hydrodynamics, how they might influence socioeconomic activities, and the assessment of the area's suitability for different activities, following the approach of [14].

The points and sections that still displayed values beyond the optimal threshold by the end of the attempts were consistently associated with two limitations: proximity to open boundaries and insufficient in situ bathymetric data (e.g., P3 and P10; CS6), with both of which are responsible for increasing error in hydrodynamic simulations [20]. The latter, in particular, reveals how a low density of morphological data propagates error in complex estuarine domains, as also displayed by [49].

Bathymetry emerged as a highly influential calibration parameter, aligning with the notion that estuarine hydrodynamic models are more sensitive to bathymetric errors compared to roughness [43,49,50]. Deepening the Guamá River by 2 m (V5) overestimated the volume transported during the high-discharge period, while a 1 m depth reduction in iteration V6 substantially improved river discharge representation by the Acará and Guamá rivers. Many of these necessary corrections resulted from sparse data in these regions, requiring greater interpolation, which can introduce systematic errors in channel depth and cross-sectional geometry—both of which directly affect tidal propagation and discharge volume. The bathymetric corrections applied during calibration (V3, V5, V6) should therefore be understood partly as compensations for interpolation uncertainty rather than purely as physical refinements. These results highlight how the acquisition of high-resolution, accurate local bathymetric data is indispensable for credible hydrodynamic modeling, as also mentioned by [51].

Bathymetry calibration was usually accompanied by increases in discharge values. Discharge measuring stations in the study area are few and far between, with large gaps in their time series. This reduces the quantity of reliable, available data, requiring the

application of scaling factors to account for distance between the chosen station and the river boundary—since river discharge increases downstream as it receives contributions from several tributaries [52]—as well as for intrinsic boundary errors. These scaling factors carry inherent uncertainty, and residual mismatches between estimated and actual boundary discharge likely contributed to the errors observed.

Sections CS12 to CS14, corresponding to Furo do Arrozal, also illustrate another constraint, arising from the large scale of the model. Despite the great density of bathymetric data, the area is composed of several small channels [53] that were not included in this simulation. Omitting tributary channels reduces the total discharge, which is consistent with the lower simulated discharge observed at CS12–CS14, especially noted in high-discharge scenarios (Figure A3), when the contribution of tributaries is higher [52]. This simplification was necessary given the spatial scale of the model and the associated computational constraints, but they set a practical lower bound on achievable accuracy in those areas particularly sensitive to local dynamics, as opposed to being influenced by the Pará River Estuary [42].

Similarly, it is important to note that the model domain does not explicitly represent floodplain inundation. Excluding the floodplain–channel exchange removes a significant storage and attenuation mechanism that influences discharge timing and magnitude, particularly during high-discharge or transitional periods (Figures A2 and A4). However, as the study did not intend to analyze such interactions and calibration indices suggested satisfactory agreement without them, this simplification was, once again, made in favor of computational efficiency. Nevertheless, these findings underscore the importance of nested or high-resolution sub-models in environmentally sensitive zones, such as this one [54], which are common throughout the Amazon region, either due to frequent flood events or due to anthropogenic pressures. In such cases, the exclusion of floodplains or channel networks might underestimate risks or make satisfactory analysis impossible.

Tidal amplitude also emerged as a highly influential parameter, consistent with previous studies that highlighted the major influence of tides on the study region [31]. A 0.3 m adjustment to the M2 component reduced errors up to 10% in the Furo do Arrozal region, whereas previous tests—where only river discharge was altered—did not yield such substantial results. Another modification involved replacing the harmonics generated by the TPXO 7.2 model at the northern boundary with those derived from observed data, which significantly enhanced model results. The improvement resulting from this action is attributed to the scarcity of data for the study region within the previously used model [55,56].

Global tidal models are widely used in hydrodynamic applications, but their skill often decreases in estuaries and nearshore zones, where complex bathymetry and coastline geometry require higher spatial resolution [57,58]. Although tools such as TPXO incorporate gauge data in some regions, coverage remains limited along large portions of the Amazon coast. For this study area, replacing the TPXO-based boundary forcing with locally derived harmonics improved tidal propagation and reduced overall error, indicating that regionalization of boundary conditions is essential for reliable predictions in macrotidal Amazonian systems, considering their morphological complexity.

Previous studies in the area had successfully implemented the TPXO 7.2 model as a tidal boundary in both the northern and southern limits of this region [28]. However, the former extended further towards the ocean, reaching zones with greater model resolution than those available for this study's domain. The TPXO harmonics were retained at the southern boundary because of lack of local water level data for that region and due to their previously demonstrated skill there but replaced at the northern boundary where it was deemed insufficient for adequately simulating local hydrodynamics. This decision likely

contributed to the residual errors observed at stations near this boundary and suggests that implementing both boundaries with local data would yield better results.

5. Conclusions

The vast spatial extent and intricate network of rivers and tidal channels that characterize Amazonian estuarine systems make their hydrodynamic representation inherently challenging. This study demonstrated that even small channels can have a substantial influence on local hydrodynamics and that accurate simulations depend fundamentally on the integration of high-resolution regional data.

Tidal harmonics and bathymetry were the most influential parameters controlling model performance, with bathymetric representation exerting a stronger effect on river discharge than bed roughness. The initial adoption of a low-density global tidal dataset increased the global simulation error in both the analysis of free surface elevation and volume transport, whereas the incorporation of locally collected data substantially reduced such errors and improved reliability.

Remaining mismatches were largely associated with proximity to open boundaries and areas with sparse in situ bathymetric data. These limitations reinforce the importance of adequate domain extension and continuous local surveying efforts, particularly in large domains where model skill depends on the availability of regional observations. In the Furo do Arrozal region, errors attributed to the exclusion of tributary channels from the modeled network highlight the need to assess, case by case, whether adjacent channels and floodplains should be represented explicitly to achieve greater simulation accuracy without excessive computational cost.

Overall, the calibrated model reproduces the dominant hydrodynamic processes of the study area, contributes to improving the hydrodynamic representation of macrotidal Amazonian estuaries and provides a basis for coastal and estuarine management applications in the Belém metropolitan region, including water quality assessments and studies of contaminants and floating-litter dispersion. Furthermore, it provides a transferable calibration framework to achieve a well-calibrated hydrodynamic model in complex tropical estuaries, contributing to the coastal management of the Amazonian region as a whole.

Author Contributions: A.H.B.Q.: conceptualization; methodology, validation, investigation, writing—original draft preparation; writing—review and editing. M.A.V.C.: methodology; methodology, validation, investigation, writing—review and editing; supervision. I.V.G.B.: methodology, validation, investigation. T.A.d.C.B.: supervision; validation; writing—review and editing. M.R.: writing—review and editing; supervision; resources; project administration; funding acquisition. All authors have read and agreed to the published version of the manuscript.

Funding: This work was supported by the National Council for Scientific and Technological Development (CNPq) [grant Number 149402/2024-4].

Data Availability Statement: The data presented in this study are available on request from the corresponding author.

Acknowledgments: The authors would like to thank the Amazon Coast Observatory (OCA) for providing the data used in this study.

Conflicts of Interest: The authors declare no conflicts of interest.

Appendix A

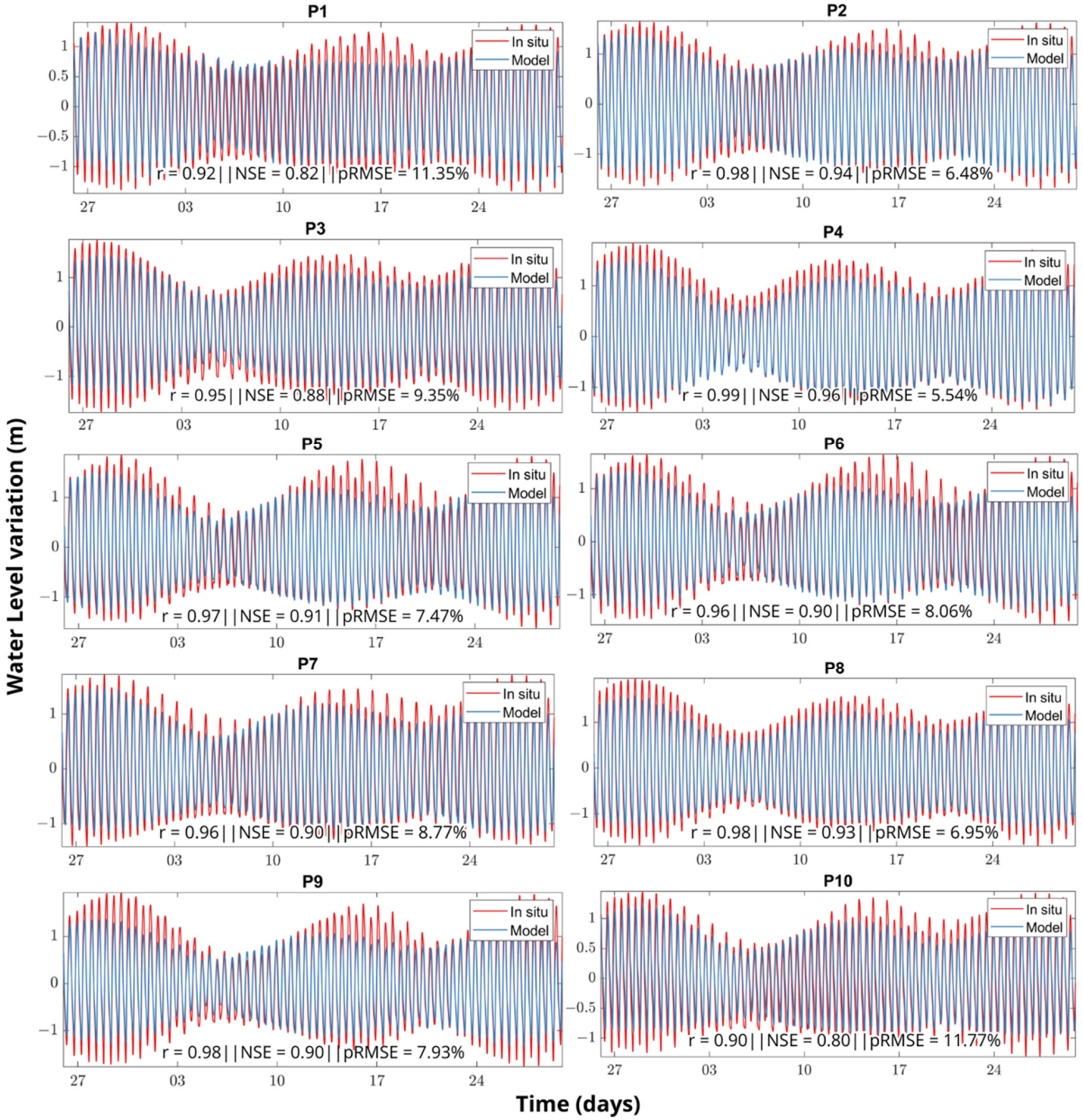


Figure A1. Final validation curves and indices for water level variation in S4 for points 1 through 10.

Appendix B

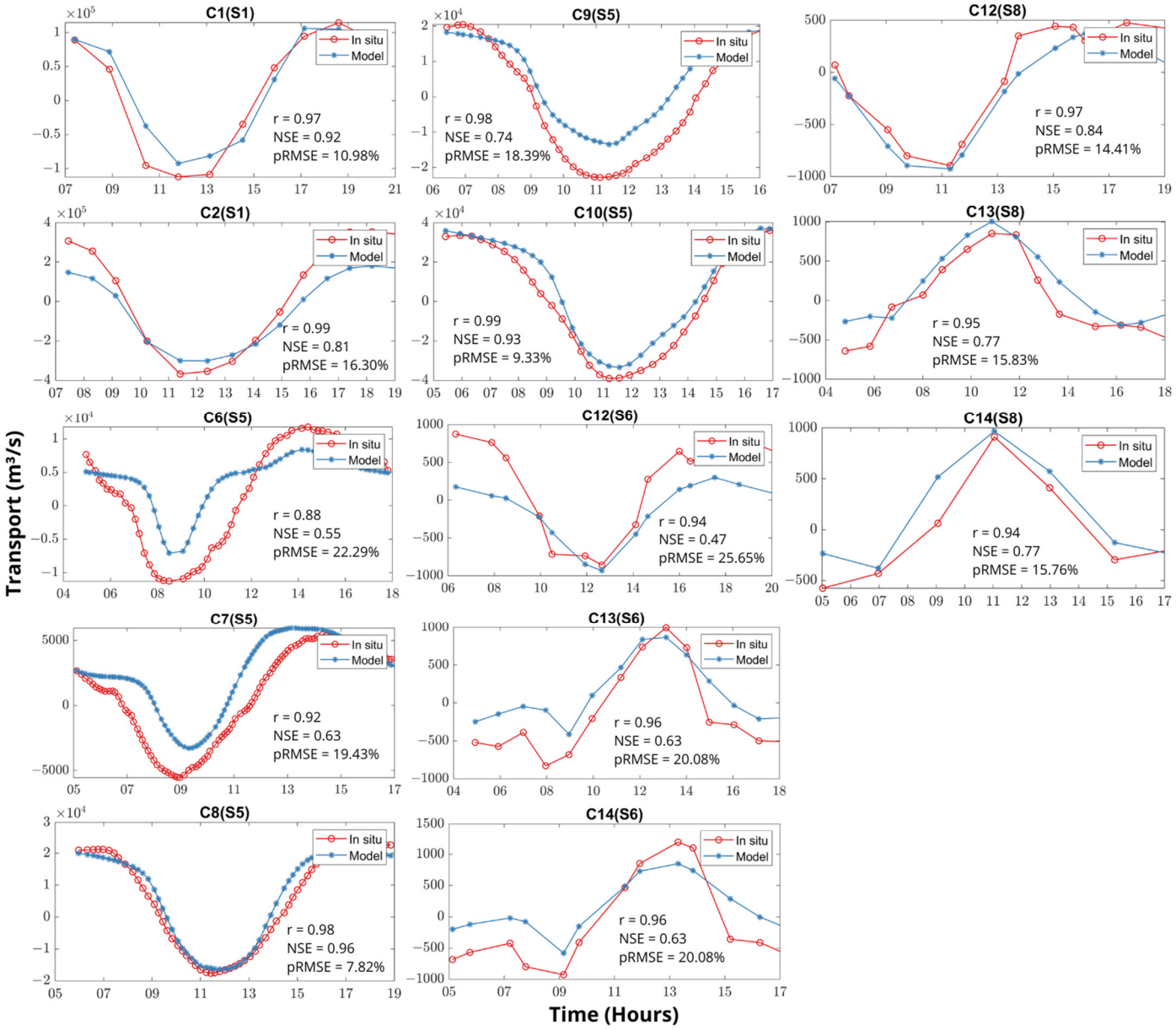


Figure A2. Final validation curves and indices for volume transported in scenarios of transitional river discharge values (S1, S5, S6 and S8).

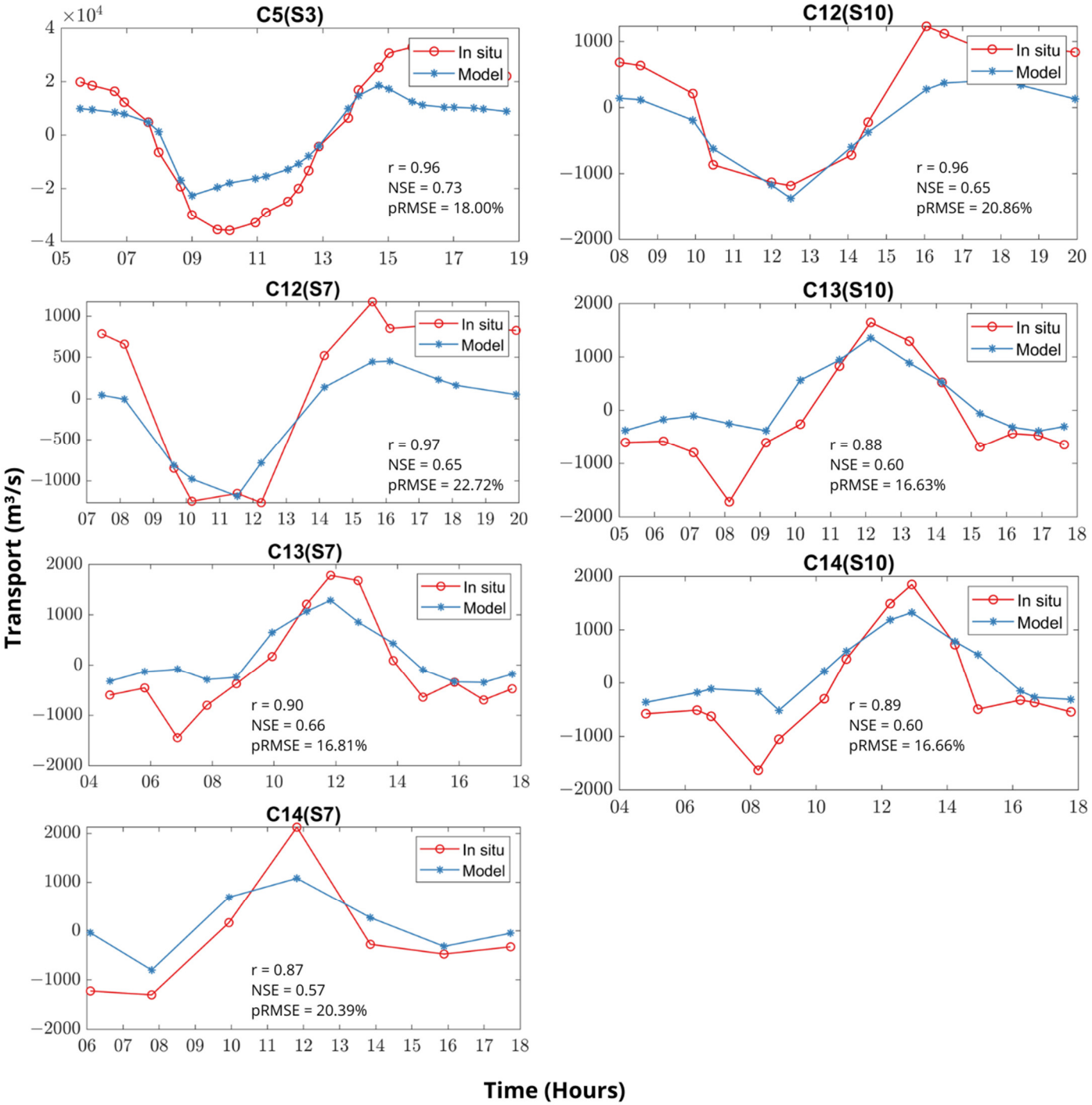


Figure A3. Final validation curves and indices for volume transported in scenarios of high river discharge values (S3, S7 and S10).

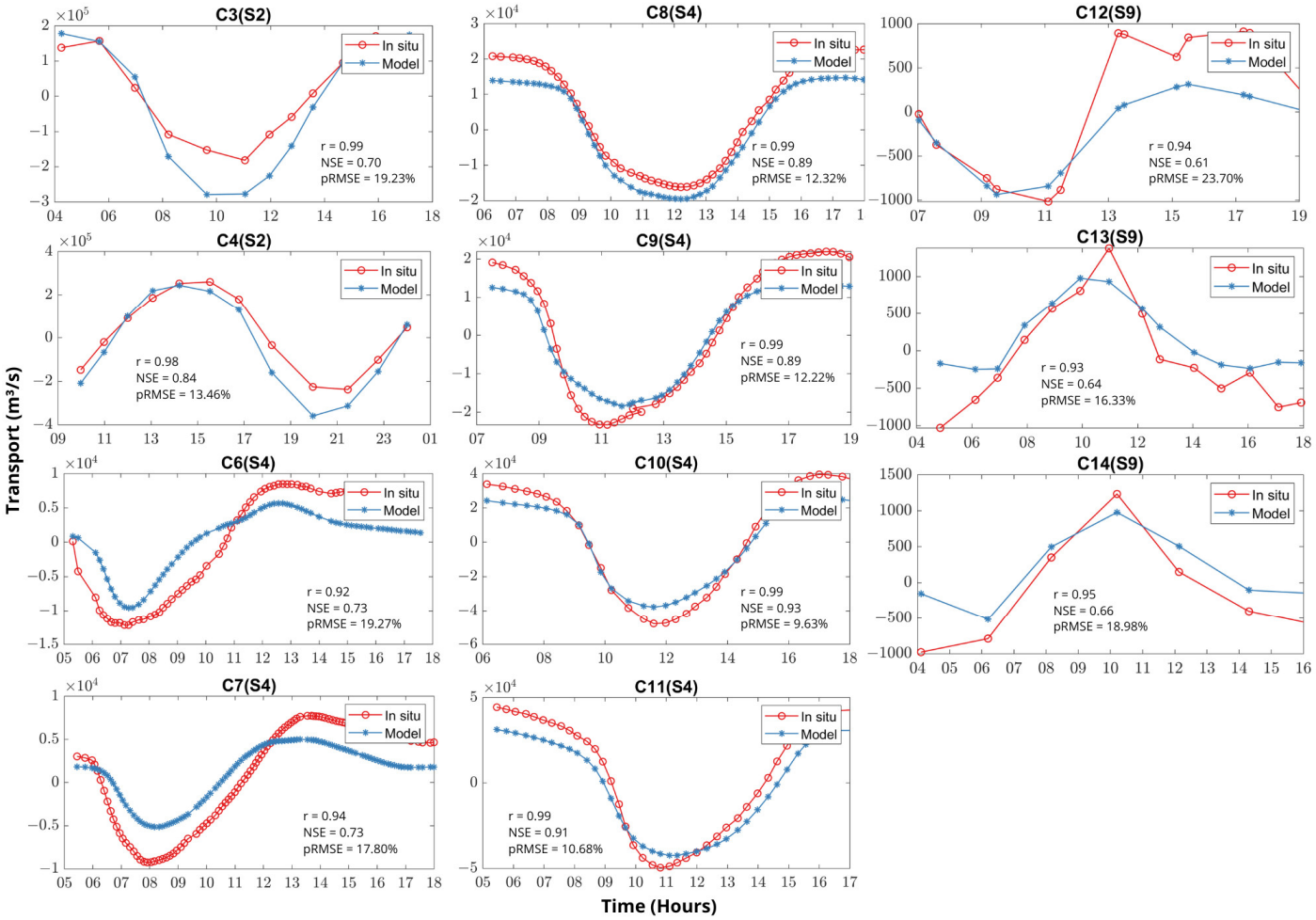


Figure A4. Final validation curves and indices for volume transported in scenarios of low river discharge values (S2, S4 and S9).

References

1. Jenkins, C.N.; Athayde, S.; Beveridge, C.F.; Correa, S.B.; Espinoza, J.C.; Heilpern, S.A.; Herrera-R, G.A.; Victoria-Lacy, L.L.; Olivas, P.; Oliveira, A.; et al. Global Importance of Amazonian Freshwaters. *Front. Ecol. Environ.* **2025**, *23*, e2868. [CrossRef]
2. Crizanto, J.L.P.; de Abreu, C.H.M.; de Souza, E.B.; da Cunha, A.C. Modeling the Impacts of Sea Level Rise Scenarios on the Amazon River Estuary. *Hydrology* **2024**, *11*, 86. [CrossRef]
3. Junk, W.J. Ecology, Fisheries and Fish Culture in Amazonia. In *The Amazon: Limnology and Landscape Ecology of a Mighty Tropical River and Its Basin*; Sioli, H., Ed.; Springer: Dordrecht, The Netherlands, 1984; pp. 443–476, ISBN 978-94-009-6542-3.
4. Ribas, C.C.; Sawakuchi, A.O.; de Almeida, R.P.; Pupim, F.N.; Rego, M.A.; Batista, R.; Knowles, L.L. The Role of Rivers in the Origin and Future of Amazonian Biodiversity. *Nat. Rev. Biodivers.* **2025**, *1*, 14–31. [CrossRef]
5. de Oliveira Agra, K.L. Social Issues in Amazon Waters: Senses, Perceptions and Representations. *Acta Sci. Hum. Soc. Sci.* **2017**, *39*, 187. [CrossRef]
6. Formigosa, M.M.; Albanese, V. Navegando por las Matemáticas Ribereñas: Sistemas de Orientación Locales en las Comunidades del Río Xingú. *Acta Sci.* **2025**, *27*, 1–24. [CrossRef]
7. Harris, M. The Rhythm of Life on the Amazon Floodplain: Seasonality and Sociality in a Riverine Village. *J. R. Anthropol. Inst.* **1998**, *4*, 65. [CrossRef]
8. Sinclair, J.L. Hydrodynamic Modeling. In *Circulating Fluidized Beds*; Springer: Dordrecht, The Netherlands, 1997; pp. 149–180. [CrossRef]
9. Wright, K.A.; Goodman, D.H.; Som, N.A.; Alvarez, J.; Martin, A.; Hardy, T.B. Improving Hydrodynamic Modelling: An Analytical Framework for Assessment of Two-Dimensional Hydrodynamic Models. *River Res. Appl.* **2017**, *33*, 170–181. [CrossRef]
10. Hendrickx, G.G.; Antolínez, J.A.A.; Herman, P.M.J. Predicting the Response of Complex Systems for Coastal Management. *Coast. Eng.* **2023**, *182*, 104289. [CrossRef]

11. Castro-Rosero, L.M.; Hernandez, I.; Alsina, J.M.; Espino, M. Transport and Accumulation of Floating Marine Litter in the Black Sea: Insights from Numerical Modeling. *Front. Mar. Sci.* **2023**, *10*, 1213333. [CrossRef]
12. Zacharias, I.; Gianni, A. Hydrodynamic and Dispersion Modeling as a Tool for Restoration of Coastal Ecosystems. Application to a Re-Flooded Lagoon. *Environ. Model. Softw.* **2008**, *23*, 751–767. [CrossRef]
13. Keramea, P.; Spanoudaki, K.; Zodiatis, G.; Gikas, G.; Sylaios, G. Oil Spill Modeling: A Critical Review on Current Trends, Perspectives, and Challenges. *J. Mar. Sci. Eng.* **2021**, *9*, 181. [CrossRef]
14. Hermawan, S.; Bangguna, D.; Mihardja, E.; Fernaldi, J.; Prajogo, J.E. The Hydrodynamic Model Application for Future Coastal Zone Development in Remote Area. *Civ. Eng. J.* **2023**, *9*, 1828–1850. [CrossRef]
15. da Silva, P.D.; Fernandes, E.H.; Gonçalves, G.A. Sustainable Development of Coastal Areas: Port Expansion with Small Impacts on Estuarine Hydrodynamics and Sediment Transport Pattern. *Water* **2022**, *14*, 3300. [CrossRef]
16. Venancio, K.K.; Garcia, P.D.; Gireli, T.Z.; Corrêa, T.B. Hydrodynamic Modeling with Scenario Approach in the Evaluation of Dredging Impacts on Coastal Erosion in Santos (Brazil). *Ocean Coast. Manag.* **2020**, *195*, 105227. [CrossRef]
17. Cerralbo, P.; Pedrera Balsells, M.F.; Mestres, M.; Fernandez, M.; Espino, M.; Grifoll, M.; Sanchez-Arcilla, A. Use of a Hydrodynamic Model for the Management of Water Renovation in a Coastal System. *Ocean Sci.* **2019**, *15*, 215–226. [CrossRef]
18. Seenath, A.; Wilson, M.; Miller, K. Hydrodynamic versus GIS Modelling for Coastal Flood Vulnerability Assessment: Which Is Better for Guiding Coastal Management? *Ocean Coast. Manag.* **2016**, *120*, 99–109. [CrossRef]
19. Teeter, A.M.; Johnson, B.H.; Berger, C.; Stelling, G.; Scheffner, N.W.; Garcia, M.H.; Parchure, T.M. Hydrodynamic and Sediment Transport Modeling with Emphasis on Shallow-Water, Vegetated Areas (Lakes, Reservoirs, Estuaries and Lagoons). *Hydrobiologia* **2001**, *444*, 1–23. [CrossRef]
20. Williams, J.J.; Esteves, L.S. Guidance on Setup, Calibration, and Validation of Hydrodynamic, Wave, and Sediment Models for Shelf Seas and Estuaries. *Adv. Civ. Eng.* **2017**, *2017*, 5251902. [CrossRef]
21. Asp, N.E.; Amorim de Freitas, P.T.; Gomes, V.J.C.; Gomes, J.D. Hydrodynamic Overview and Seasonal Variation of Estuaries at the Eastern Sector of the Amazonian Coast. *J. Coast. Res.* **2013**, *165*, 1092–1097. [CrossRef]
22. Prestes, Y.O.; da Costa Borba, T.A.; da Silva, A.C.; Rollnic, M. A Discharge Stationary Model for the Pará-Amazon Estuarine System. *J. Hydrol. Reg. Stud.* **2020**, *28*, 100668. [CrossRef]
23. da Silva Gregório, A.M.; Carvalho Mendes, A. Batimetria e sedimentologia da Baía de Guajará, Belém, estado do Pará, Brasil. *Amazon. Cien. Desenvolv.* **2009**, *5*, 53.
24. Bezerra, M.O.; Medeiros, C.; Krelling, A.P.M.; Rosário, R.P.; Rollnic, M. Physical Oceanographic Behavior at the Guama/Acara-Moju and the Paracauari River Mouths, Amazon Coast (Brazil). *J. Coast. Res.* **2011**, *SI(64)*, 1448–1452.
25. de Andrade, V.M.S.; Cordeiro, I.M.C.C.; Schwartz, G.; Rangel-Vasconcelos, L.G.T.; de Oliveira, F.A. Considerações Sobre Clima e Aspectos Edafoclimáticos da Mesorregião Nordeste Paraense. In *Nordeste Paraense: Panorama Geral e Uso Sustentável das Lorestas Secundárias*; EDUFRA: Belém, Brazil, 2017; pp. 59–96.
26. Bastos, T.X.; Pacheco, N.A.; Nechet, D.; de Sá, T.D.A. *Aspectos Climáticos de Belém Nos Últimos Cem Anos*; Documentos, 128; Embrapa Amazônia Oriental: Belém, Brazil, 2002.
27. Deltares. *D-Flow Flexible Mesh*; User Manual; Deltares: Delft, The Netherlands, 2026.
28. Borba, T.; Roelvink, D.; Rollnic, M. Hydrodynamic Modelling in the Amazonian Estuary: A Flexible Mesh Approach. *Ocean Coast. Res.* **2025**, *73*, e25020. [CrossRef]
29. Borba, T.A.C.; Rollnic, M. Runoff Quantification on Amazonian Estuary Based on Hydrodynamic Model. *J. Coast. Res.* **2016**, *1*, 43–47. [CrossRef]
30. Arcement, G.J.; Schneider, V.R. Guide for Selecting Manning's Roughness Coefficients for Natural Channels and Flood Plains. *Water Supply Pap.* **1989**, *38*, ill. [CrossRef]
31. Prestes, Y.O.; Silva, A.C.; Rollnic, M.; Rosário, R.P. The M2 And M4 Tides in the Pará River Estuary. *Trop. Oceanogr.* **2017**, *45*, 26–37. [CrossRef]
32. Pereira, D.R.; Oliveira, A.R.; Costa, M.S.; Rollnic, M.; Neves, R. Simulation of Tidal Oscillations in the Pará River Estuary Using the MOHID-Land Hydrological Model. *Water* **2025**, *17*, 1048. [CrossRef]
33. Kubota, N.A.; Lima, A.M.M.D.; Rocha, N.C.V.; Lima, I.F. Hidrogeomorfologia da Bacia Hidrográfica do rio Guamá-Amazônia Oriental-Brasil. *Rev. Bras. Geomorfol.* **2020**, *21*, 759–782. [CrossRef]
34. Monteiro Neto, A.; da Cost Barbosa, I.C.; dos Santos, A.M.; de Melo Menezes, P.M.; Fiel, L.G.; de Sousa, M.C.; Batista, L.M.; de Lima Rodrigues, R.R.; da Silva Costa, I.C. Análise Multicritérios Como Ferramenta de Identificação de Áreas Aptas à Expansão Da Dendeicultura Na Bacia Hidrográfica Do Rio Acará, PA. *Rev. Ibero-Am. Cienc. Ambient.* **2021**, *12*, 584–607. [CrossRef]
35. Ferreira, S.C.G.; Lima, A.M.M.d.; Corrêa, J.A.M. Zoneamento Da Bacia Hidrográfica Do Rio Moju (Pará): Usos Da Água e Sua Relação Com as Formas de Uso e Cobertura Do Solo. *Rev. Ambiente Água* **2017**, *12*, 680–693. [CrossRef]
36. M. de Abreu, C.H.; Barros, M.d.L.C.; Brito, D.C.; Teixeira, M.R.; Cunha, A.C.d. Hydrodynamic Modeling and Simulation of Water Residence Time in the Estuary of the Lower Amazon River. *Water* **2020**, *12*, 660. [CrossRef]

37. Moriasi, D.N.; Gitau, M.W.; Pai, N.; Daggupati, P. Hydrologic and Water Quality Models: Performance Measures and Evaluation Criteria. *Trans. ASABE* **2015**, *58*, 1763–1785. [CrossRef]
38. Moriasi, D.N.; Arnold, J.G.; Liew, M.W.V.; Bingner, R.L.; Harmel, R.D.; Veith, T.L. Model Evaluation Guidelines for Systematic Quantification of Accuracy in Watershed Simulations. *Trans. ASABE* **2007**, *50*, 885–900. [CrossRef]
39. Matte, P.; Secretan, Y.; Morin, J. Hydrodynamic Modeling of the St. Lawrence Fluvial Estuary. I: Model Setup, Calibration, and Validation. *J. Waterw. Port. Coast. Ocean Eng.* **2017**, *143*, 04017010. [CrossRef]
40. Gupta, H.V.; Kling, H.; Yilmaz, K.K.; Martinez, G.F. Decomposition of the Mean Squared Error and NSE Performance Criteria: Implications for Improving Hydrological Modelling. *J. Hydrol.* **2009**, *377*, 80–91. [CrossRef]
41. Ferreira, D.M.; Fernandes, C.V.S.; Kaviski, E.; Bleninger, T. Calibration of River Hydrodynamic Models: Analysis from the Dynamic Component in Roughness Coefficients. *J. Hydrol.* **2021**, *598*, 126136. [CrossRef]
42. Barros, M.D.L.C.; Goulart Pecly, J.O.; S. Lima, L.; Neu, V.; Richey, J.E.; CC Rosman, P. Influence of Boundary Condition Uncertainties on Hydrodynamic Simulations. *Model. Earth Syst. Environ.* **2025**, *11*, 368. [CrossRef]
43. Khanarmuei, M.; Suara, K.; Sumihar, J.; Brown, R.J. Hydrodynamic Modelling and Model Sensitivities to Bed Roughness and Bathymetry Offset in a Micro-Tidal Estuary. *J. Hydroinform.* **2020**, *22*, 1536–1553. [CrossRef]
44. Okon, L.-U.E.; Seelam, J.K.; Hemanath, L.; Thomas, J.; Narine, R. Hypothesis-Driven Sensitivity Analysis of Delft3D Flexible Mesh Hydrodynamic Model: Insights into Coastal Processes in the Monsoonal Tropical Goa Coast, India. *Ocean Dyn.* **2025**, *75*, 79. [CrossRef]
45. Hyde, J.L.; Swanson, C.; Bohlman, S.A.; Athayde, S.; Bruna, E.M.; Valle, D.R. A Lack of Open Data Standards for Large Infrastructure Projects Hampers Social-Ecological Research in the Brazilian Amazon. *PeerJ* **2025**, *13*, e19926. [CrossRef]
46. Reis, L.N.D.; Polidori, L. Challenges of Relief Modeling in Flat Areas: A Case Study in the Amazon Coast Floodplains. *Bol. Cienc. Geod.* **2024**, *30*, e2024009. [CrossRef]
47. Munizaga, J.; García, M.; Ureta, F.; Novoa, V.; Rojas, O.; Rojas, C. Mapping Coastal Wetlands Using Satellite Imagery and Machine Learning in a Highly Urbanized Landscape. *Sustainability* **2022**, *14*, 5700. [CrossRef]
48. Sampurno, J.; Vallaeys, V.; Ardianto, R.; Hanert, E. Integrated Hydrodynamic and Machine Learning Models for Compound Flooding Prediction in a Data-Scarce Estuarine Delta. *Nonlinear Process. Geophys.* **2022**, *29*, 301–315. [CrossRef]
49. Cea, L.; French, J.R. Bathymetric Error Estimation for the Calibration and Validation of Estuarine Hydrodynamic Models. *Estuar. Coast. Shelf Sci.* **2012**, *100*, 124–132. [CrossRef]
50. Brakenhoff, L.; Schrijvershof, R.; van der Werf, J.; Grasmeijer, B.; Ruessink, G.; van der Vegt, M. From Ripples to Large-Scale Sand Transport: The Effects of Bedform-Related Roughness on Hydrodynamics and Sediment Transport Patterns in Delft3D. *J. Mar. Sci. Eng.* **2020**, *8*, 892. [CrossRef]
51. Bars, Y.L.; Lyard, F.; Jeandel, C.; Dardengo, L. The AMANDES Tidal Model for the Amazon Estuary and Shelf. *Ocean Model.* **2010**, *31*, 132–149. [CrossRef]
52. Freitas, P.T.A.; Silveira, O.F.M.; Asp, N.E. Tide Distortion and Attenuation in an Amazonian Tidal River. *Braz. J. Oceanogr.* **2012**, *60*, 429–446. [CrossRef]
53. Simão, C.d.S.; El-Robrini, M.; Santos, M.d.L.S.; da Silva, N.M. Influência Da Sazonalidade Sobre as Águas Estuarinas de Um Furo Amazônico (Arrozal—Barcarena, Pará, Amazônia Oriental). *Geografia* **2025**, *50*, 512–539. [CrossRef]
54. Rodrigues, R.D.M. Quando falam os rios da Amazônia: Quem são e como são produzidos os atingidos por grandes projetos em Barcarena, no Pará. *Nova Rev. Amaz.* **2024**, *12*, 123–136. [CrossRef]
55. Daher, V.B. Refinamento de Dados de Altimetria por Satélite Medidos ao Longo da Costa Brasileira. Ph.D. Thesis, Federal University of Rio de Janeiro, Rio de Janeiro, Brazil, 2019; p. 108.
56. Egbert, G.D.; Erofeeva, S.Y. Efficient Inverse Modeling of Barotropic Ocean Tides. *J. Atmos. Ocean. Technol.* **2002**, *19*, 183–204. [CrossRef]
57. Sun, W.; Zhou, X.; Zhou, D.; Sun, Y. Advances and Accuracy Assessment of Ocean Tide Models in the Antarctic Ocean. *Front. Earth Sci.* **2022**, *10*, 757821. [CrossRef]
58. Stammer, D.; Ray, R.D.; Andersen, O.B.; Arbic, B.K.; Bosch, W.; Carrère, L.; Cheng, Y.; Chinn, D.S.; Dushaw, B.D.; Egbert, G.D.; et al. Accuracy Assessment of Global Barotropic Ocean Tide Models. *Rev. Geophys.* **2014**, *52*, 243–282. [CrossRef]

Disclaimer/Publisher's Note: The statements, opinions and data contained in all publications are solely those of the individual author(s) and contributor(s) and not of MDPI and/or the editor(s). MDPI and/or the editor(s) disclaim responsibility for any injury to people or property resulting from any ideas, methods, instructions or products referred to in the content.